Acta Cryst. (1958). **11**, 61

The Crystal Structure of Ammonium Hydrogen D-Tartrate

BY A. J. VAN BOMMEL* AND J. M. BIJVOET

Laboratorium voor Kristalchemie der Rijks-Universiteit, Utrecht, Netherlands

(*Received* 7 *June* 1957)

The structure of NH_4–H-tartrate has been determined by means of a three-dimensional analysis. The crystals are orthorhombic with $a = 7{\cdot}648$, $b = 11{\cdot}066$, $c = 7{\cdot}843$ Å; space group $P2_12_12_1$; 4 molecules per unit cell. Accurate intensities were obtained by Geiger-counter measurements. The atomic coordinates and anisotropic temperature-factor parameters were calculated by least-squares methods and from three-dimensional difference Fourier maps. Bond lengths and electron densities have been measured with standard deviations of 0·004 Å and 0·1 e.Å^{-3} respectively. The positions of the hydrogen atoms have been determined. No indication of the binding electrons was found. The absolute configuration of Rb–H-tartrate proves to be in accordance with the previously determined configuration from Rb–Na-D-tartrate.

Introduction

Some years ago we determined the absolute configuration of the tartaric acid molecule from the Rb–Na-tartrate. In order to test this result by means of a more accurately determined structure, we started the investigation of the isomorphous series Rb–H-tartrate, K–H-tartrate and NH_4–H-tartrate to obtain more accurate atomic coordinates from the lighter NH_4 compound and to introduce these into Rb–H-tartrate.

During the investigation of the NH_4 salt our interest was focused on the refinement of this non-centrosymmetrical structure in a three-dimensional analysis based on Geiger-counter measurements.

Two-dimensional analysis

Crystals of Rb–, K– and NH_4–H-D-tartrates were obtained by cooling a solution of these salts, saturated at 50° C. The crystals are elongated prisms in the [100] direction, and belong to the orthorhombic disphenoidal crystal class (Groth, 1906–19).

The cell dimensions of the Rb and NH_4 compounds were calculated from the zero layer lines of rotation diagrams about [100] and [001], those of the K compound were obtained from layer-line distances:

Rb–H-tartrate

$a = 7{\cdot}665$, $b = 10{\cdot}980$, $c = 7{\cdot}917$ Å, all $\pm 0{\cdot}003$ Å;
$U = 666{\cdot}3$ Å^3; $D_m = 2{\cdot}29$ g.cm.$^{-3}$, $D_x = 2{\cdot}33$ g.cm.$^{-3}$;
$Z = 4$.

K–H-tartrate

$a = 7{\cdot}64$, $b = 10{\cdot}62$, $c = 7{\cdot}75$ Å, all $\pm 0{\cdot}02$ Å;
$U = 629$ Å^3; $D_m = 1{\cdot}96$ g.cm.$^{-3}$, $D_x = 1{\cdot}99$ g.cm.$^{-3}$;
$Z = 4$.

NH_4–H-tartrate

$a = 7{\cdot}648$, $b = 11{\cdot}066$, $c = 7{\cdot}843$ Å, all $\pm 0{,}003$ Å;
$U = 663{\cdot}8$ Å^3; D_m; $= 1{\cdot}68$ g.cm.$^{-3}$, $D_x = 1{\cdot}69$ g.cm.$^{-3}$
$Z = 4$.

The space group $P2_12_12_1$ follows from the systematic absences. Intensity data for the $hk0$ and $0kl$ reflexions were recorded with Cu $K\alpha$ radiation on zero-level Weissenberg films about the a and c axes by the multiple-film technique (Lange, Robertson & Woodward, 1939) and estimated by visual comparison with an intensity scale. The crystals were ground to the shape of a cylinder with a cross section of 0·2 mm. In the case of the Rb and K compound, absorption was corrected for. Corrections for Lorentz and polarization factors were applied and the observed structure amplitudes were brought to an absolute scale in a later stage of the analysis by scaling against the calculated values.

Structure determination from the a and c projections

Patterson projections along the a and c axes were constructed for Rb–H-tartrate. Since the space group $P2_12_12_1$ contains only fourfold general positions, Rb–Rb vectors occur at

$2y, \frac{1}{2}; \frac{1}{2}, \frac{1}{2}-2z; \frac{1}{2}-2y, 2z$ for the a-axis projection

and

$\frac{1}{2}, \frac{1}{2}-2y; 2x, \frac{1}{2}; \frac{1}{2}-2x, 2y$ for the c-axis projection.

Corresponding to these vector sets, each Patterson projection showed three heavy peaks, giving for the Rb coordinates

$$x = 0{\cdot}917, \quad y = 0{\cdot}217, \quad z = 0{\cdot}081 .$$

The corresponding Fourier projections were synthesized, using the signs of the Fourier coefficients given

* Now at the Natuurkundig Laboratorium der N. V. Philips' Gloeilampenfabrieken, Eindhoven, Netherlands.

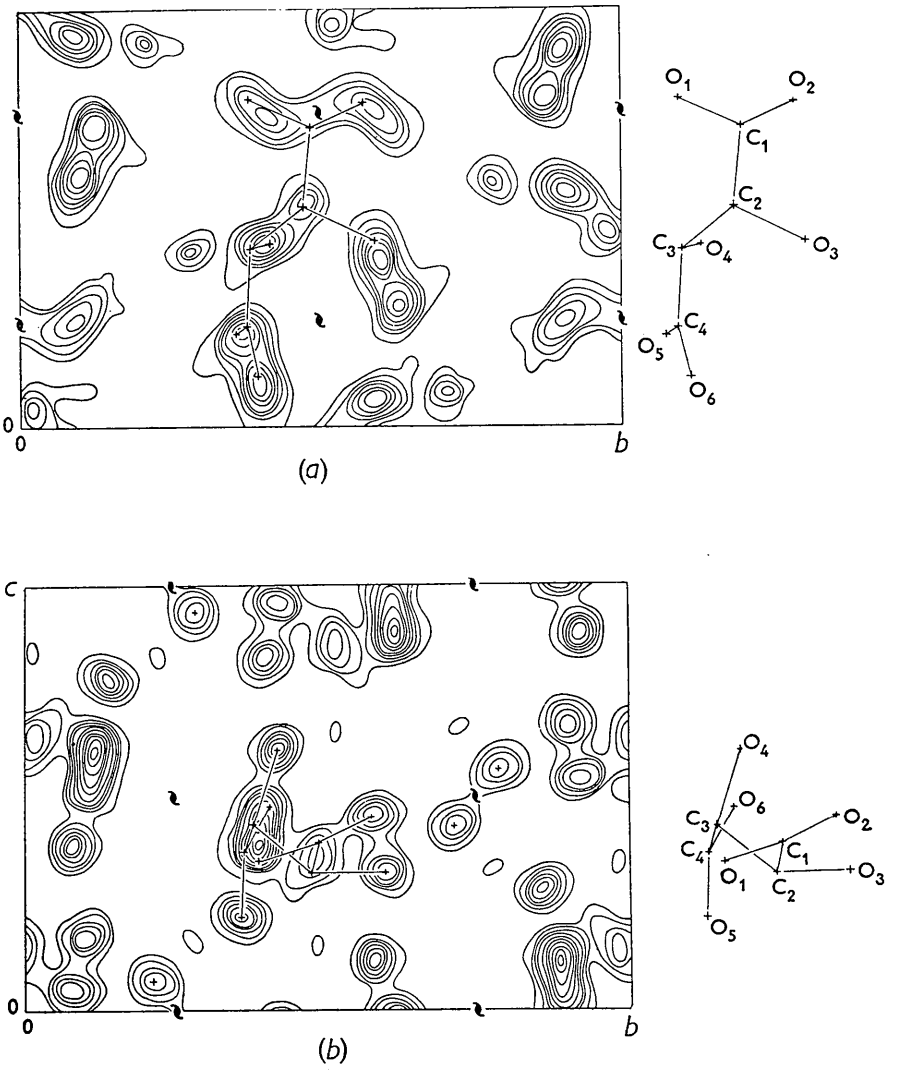

Fig. 1. Electron density of NH_4–H-tartrate projected (*a*) on (100), (*b*) on (001). Contours are drawn at equal intervals on an arbitrary scale.

by the heavy-atom contribution. The Fouriers showed a considerable overlap of the atomic peaks, but by using a model of tartaric acid it proved possible to determine the coordinates of the O, C and N atoms. These coordinates were used in the calculation of the signs of the structure factors of the isomorphous K and NH_4 salts. The Fourier maps of these salts also showed a considerable overlap (Fig. 1). We therefore decided to find the accurate coordinates of NH_4–H-tartrate from a three-dimensional analysis. With this analysis in view, the coordinates found from the *a* and *c* Fourier projections in NH_4–H-tartrate, were refined by a least-squares method minimizing

$$R_1 = \sum_n (F_o - F_c)^2 .$$

Here $\sum_n$ denotes a summation over all observed reflexions. In F_c a temperature factor $\exp[-B\sin^2\theta/\lambda^2]$ was applied with $B = 1{\cdot}5$ Å^2, deduced from the ratio $|F_o| \div |F_c|$ against $\sin^2\theta$. Table 1 gives the atomic coordinates of NH_4–H-tartrate from which we started the three-dimensional analysis.

Table 1. *Atomic coordinates of* NH_4–H-*tartrate. determined from the* [100] *and* [001] *projections*

	x	*y*	*z*
O_1	0·779	0·390	0·358
O_2	0·782	0·578	0·451
O_3	0·442	0·597	0·329
O_4	0·436	0·422	0·613
O_5	0·228	0·358	0·214
O_6	0·128	0·392	0·478
N	0·917	0·214	0·072
C_1	0·719	0·488	0·388
C_2	0·529	0·475	0·332
C_3	0·426	0·379	0·430
C_4	0·233	0·364	0·372

Determination of the absolute configuration of the tartaric acid from the Rb–H *compound*

The principles of the absolute-configuration determination are outlined by Bijvoet (1954) and a detailed discussion of the methods is given by Peerdeman & Bijvoet (1956). In using Zr $K\alpha$ rays, which excite the K electrons of the Rb atoms, the differences in intensity of the hkl and $hk\bar{l}$ reflexions of Table 2, column (4),

Table 2

	Calculated		Observed	
hkl	I_{hkl}	$I_{hk\bar{l}}$	I_{hkl}	$I_{hk\bar{l}}$
(1)	(2)	(3)	(4)	
113	281	351	<	
114	412	369	>	
123	371	482	<	
124	226	212	>	
125	63	52	>	
126	159	147	>	
135	227	278	<	
141	239	209	>	
143	188	149	>	
146	80	93	<	
151	359	316	>	

have been observed. The calculated relations are given in columns (2) and (3).

The Rb–H-tartrate confirms the result concerning absolute configuration deduced previously from Rb–Na-tartrate (Peerdeman, van Bommel, Bijvoet, 1951).

Three-dimensional analysis

Measurement of the integrated intensity by means of a Geiger counter

We measured the intensities by means of a Geiger counter, high accuracy being aimed at. Geiger counter measurement of single crystals in two dimensional work is well known. Cochran (1950) has examined the accuracy of such measurement.

Apparatus

We used a Bragg spectrometer which was adapted for measurements by means of a Geiger counter. The crystal mounted on a goniometer head could be oscillated around the vertical axis by a synchronous motor. The arm bearing the counter could be tilted out of the horizontal plane for measurements of higher layer lines. On two scales the position of the crystal and the counter could be read. In order to centre and adjust the specimen, the counter could readily be replaced by a microscope. With this apparatus it was possible to measure reflexions with reflexion angle of azimuth 2φ and height μ for $0° < 2\varphi < 145°$ and $-10° < \mu < 50°$.

An argon–chlorine-filled tube (Philips No. 62019) was used, connected by a coaxial cable, 60 cm. long, with the stabilized high voltage and scaler. By stabilization of the primary a.c. supply, the filament current and the tube current, the output of the X-ray tube was kept constant to within $\frac{1}{2}$% over a period of 24 hr.

Monochromatization of radiation

Besides the characteristic radiation, an X-ray beam contains a considerable amount of white radiation over a wide range of wavelength. Small ranges of this continuous spectrum, around the wavelength of the characteristic radiation used and its submultiples, will be reflected together with the characteristic radiation and hence will influence the measured intensity. As to the wavelength range $\approx \lambda$, it follows from

$$2d \sin \theta = n\lambda$$

or

$$\Delta\lambda = \frac{2d \cos \theta}{n} \Delta\theta$$

that the dispersion of the reflected radiation increases with increasing diffraction angle. The correction for this white radiation has been measured by Cochran (1950) and amounts to 6% at $2\theta = 10°$, and to less than 1% at $2\theta = 50°$.

The contribution of the wavelength $\approx \frac{1}{2}\lambda$ and $\frac{1}{3}\lambda$ can be corrected for by the balanced-filter method (Ross, 1928), but this greatly increases the amount of work. Besides, this white radiation causes a considerable background, which makes it extremely difficult to measure weak reflexions. For these reasons we used a monochromatized beam, obtained by reflexion from a bent quartz crystal. In using the $10\bar{1}1$ reflexion, the intensity of the $\frac{1}{2}\lambda$ compound is reduced to about $\frac{1}{4}$% and that of $\frac{1}{3}\lambda$ is virtually zero. Fig. 2 shows the experimental arrangement.

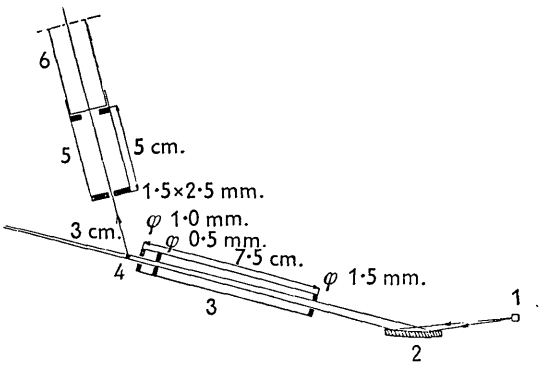

Fig. 2. Schematic drawing of the apparatus. 1: Target of the X-ray tube. 2: Bent quartz monochromator. 3: Collimator. 4: Crystal. 5: Screening slits before the counter tube. 6: Counter.

Relation between the number of counts and the integrated intensity

The number of counts recorded by the counter will not be proportional to the X-ray intensity, since any number of impulses occurring within the resolving

time, τ, of the counter will be recorded as one count. When the source produces impulses at random intervals, as in our case of a d.c.-excited X-ray tube, the number of lost counts can be calculated. Let N_0 be the number of counts recorded in 1 sec., and τ the resolving time of the counter, then the corrected number of counts in 1 sec. is given by

$$N = \frac{N_0}{1-N_0\tau} . \qquad (1)$$

In measuring the integrated reflexion intensity in the oscillating-crystal method, the reflected beam varies in intensity as the crystal passes through the reflexion range. Here the corrected number of counts of a reflexion is given by

$$M = \frac{M_0}{1-(M_0/T)\tau'} , \qquad (2)$$

where M_0 is the measured number of counts in a time T sec. and τ' is the so-called effective resolving time.

According to Cochran (1950) $\tau' = K\tau$, where

$$1/K = \frac{\text{R.m.s. reflecting power of crystal over range } \alpha}{\text{Mean reflecting power over this range}} ,$$

K can be calculated from the profile of the reflexion. It is easier, however, to determine τ' experimentally by interposing Ni foils of known absorption in the reflected beam. From the reduction factor $p = M_1/M_2$, τ' can be calculated from

$$p = \frac{\dfrac{M_{01}}{1-(M_{01}/T)\tau'}}{\dfrac{M_{02}}{1-(M_{02}/T)\tau'}} .$$

Determination of τ' for a number of strong reflexions revealed the fact that if T relates to the measurement of the reflexions from background to background, τ' proves to be a constant.

Table 3 gives the reduction factor of the measured intensity by interposing Ni foils of known absorption, for a reflexion of NH_4–H-tartrate. Column (3) gives the uncorrected values and column (5) the corrected values with $\tau = 90$ sec. and $\tau' = 225$ μ sec. A more suitable method for measuring τ' consists in determining the intensities of the strong reflexions at two different, known outputs of the X-ray tube. For a number of reflexions measured at 40 kV., 20·5 mA. and 30 kV., 10 mA. respectively, Table 4 gives the number of counts and their ratio non-corrected and corrected (columns (6) and (7) respectively). With this method it is easy to determine τ' for each crystal and each layer line.

Table 3. *Number of counts (M_0) of a reflexion and number (M) after correction*

$M = \dfrac{M_0}{1-(M_0/T)\tau'}$, with $\tau' = 225$ μ sec and $T = 90$ sec.

Number of Ni foils	M_0	$\dfrac{M_{0m}}{M_{0m+1}}$	M	$\dfrac{M_m}{M_{m+1}}$
(1)	(2)	(3)	(4)	(5)
0	117240		178817	
		1·339		1·520
1	87580		117625	
		1·376		1·505
2	63630		78136	
		1·410		1·503
3	45140		51980	
		1·450		1·519
4	31125		34230	
		1·447		1·491
5	21511		22950	
		1·476		1·508
6	14569		15215	
		1·481		1·502
7	9835		10130	
		1·455		1·469
8	6759		6895	
		1·492		1·502
9	4529		4589	
		1·525		1·532
10	2970		2996	
		1·498		1·503
11	1982		1993	
			Mean	1·505

Table 4. *Intensity of some reflexions with two different outputs of the X-ray tube*

In columns (6) and (7) the ratio before and after correction is given. $\tau' = 225$ μsec. $T = 90$ sec.

hkl	M_{01} 40 kV. 20·5 mA.	M_{02} 30 kV. 10 mA.	M_1 40 kV. 20·5 mA.	M_2 30 kV. 10 mA.	$\dfrac{M_{01}}{M_{02}}$	$\dfrac{M_1}{M_2}$
(1)	(2)	(3)	(4)	(5)	(6)	(7)
520	12292	2790	12682	2810	4·406	4·513
530	10342	2290	10616	2303	4·516	4·609
540	12680	2888	13095	2909	4·391	4·501
560	12476	2770	12877	2790	4·504	4·615
400	28156	6636	30282	6748	4·242	4·487
410	20184	4700	21256	4756	4·294	4·469
420	18940	4390	19880	4438	4·314	4·479
320	80796	21902	101248	23170	3·689	4·369
350	54246	13648	62758	14130	3·975	4·441
360	12356	2800	12750	2820	4·412	4·521
370	38126	9052	42144	9262	4·412	4·550
200	22341	5072	23662	5138	4·405	4·605
230	68104	17636	82078	18450	3·862	4·449
				Mean	4·508	

Measurement of the integrated intensity

For the measurement of the integrated intensities we used the usual oscillating-crystal method. The crystal was oscillated through the reflexion range by means of a synchronous motor. The counter was kept in the reflexion position whilst the slits shielding the counter were sufficiently wide for the whole reflexion.

The range over which the crystal had to be oscillated varied for a zero layer line from 1° at the lower reflexion angles to 1·5° at the higher reflexion angles. The angular velocity was 40′/min. so the time required for half an oscillation varied from 90 sec. to about 135 sec. In measuring higher layer lines the time of oscillation was somewhat higher.

Cu $K\alpha$ reflexions were recorded in the range $0 < \sin\theta/\lambda < 0{\cdot}63$;

Cu $K\beta$ measurements extended the range to $\sin\theta/\lambda = 0{\cdot}72$.

For every reflexion the number of counts occurring in at least one complete oscillation was recorded. For the medium strong reflexions the number of counts was more than 10^4. The statistical standard deviation

in a number of N counts being $\sqrt{N}$, we have for these reflexions a standard deviation better than 1%.

To reach this accuracy the very weak reflexions would require very large measuring times; for these unimportant reflexions, however, we took a maximum of five oscillations.

For each reading the following corrections were applied:

(1) Corrections for lost counts:

$$M = \frac{M_0}{1-(M_0/T)\tau'} .$$

(2) Correction for background: (*a*) cosmic background; (*b*) X-ray background, due to radiation scattered from the air and incoherently from the crystal itself.

For our counter the cosmic background was 40 counts/min. The total background was determined over the whole range $0° < 2\varphi < 145°$ for positions of crystal and counter beyond the reflexions. Fig. 3 gives

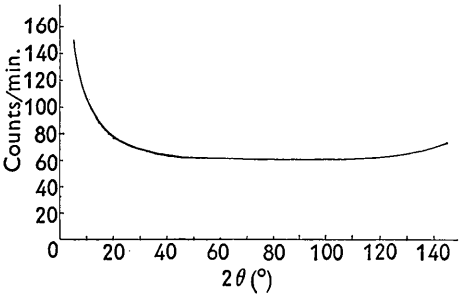

Fig. 3. Cosmic X-ray+background from a crystal of NH_4–H-tartrate. The crystal was a cylinder about [100] with a cross-section of 0·18 mm.

the measured background for a crystal of NH_4–H-tartrate. The crystal had a cross-section $d = 0{\cdot}18$ mm. and the background was measured with the X-ray tube operated at 40 kV., 20·5 mA.

(3) From the corrected intensities the F^2 values are obtained using the Lorentz and polarization factors and scale factor:

$$F^2 = CI_o/LP;$$

Lorentz factor

$$L = \frac{1}{\cos\mu \sin 2\varphi} \qquad \text{(Cochran, 1948);}$$

polarization factor

$$P = \frac{\cos^2\mu + \cos^2 2\alpha - \cos^2 2\alpha \cos^2\mu \sin^2\varphi}{1+\cos^2 2\alpha}$$

(Whittaker, 1953).

In these formulae

μ = angle of elevation of the layer line,
2φ = scattering azimuth,
2α = scattering angle of the monochromator crystal ($10\bar{1}1$ reflexion of quartz and Cu $K\alpha$ radiation, $2\alpha = 26° 44'$).

(4) The absorption correction could be omitted.

To obtain all reflexions for the three-dimensional analysis we measured *all* reflexions of the zero, first, second and third layer lines of crystals about [100], [001] and [101].

Each layer line gives the F values on an arbitrary scale. By comparison of the common reflexions all intensities were normalized to the same level and then brought on an absolute scale by the condition $\Sigma|F_o| = \Sigma|F_c|$.

Accuracy of the measurements

The statistical standard deviations in the measured intensities for all reflexions, except the very weak ones, is better than 1%. In the case of the very weak reflexions a minimum of about 1000 counts was recorded, increasing the s.d. up to 3%. Beyond the region of anomalous scattering the eight $|h||k||l|$ reflexions are equal and on each layer line two or four independent F^2 values can be measured. Comparison of these values gave a s.d. of 3% in the intensity.

An impression of the total inaccuracy in F_o, caused by errors in the measurement and in the correction factors and by the individual crystal behaviour can be obtained by comparing F_o values from different crystals and layer lines. For these common reflexions we calculated a standard deviation of 3%.

Comparison with photographic methods

Before we had a Geiger-counter equipment at our disposal, the reflexion intensities had already been obtained by photographic measurement. The reflexions were recorded on equi-inclination Weissenberg diagrams, and the intensities estimated by visual comparison with an intensity scale. After correction for Lorentz and polarization factors, the F_o values were brought to an absolute scale by comparison with F_c values. For these photographic F_o values of different crystals and layer lines the disagreement index amounts to

$$R = \Sigma||F_1|-|F_2|| \div \Sigma|F| = 0{\cdot}08 .$$

Comparison of the photographic values with the counter values gave a disagreement index:

$$R = \Sigma||F_{\text{ph.}}|-|F_{\text{ctr.}}|| \div \Sigma|F| = 0{\cdot}1 .$$

The photographic values of the strongest reflexions proved to be systematically too low.

Finally a comparison will be made between the photographic and counter measurements, as to the time required in their measurement.

The photographic diagrams were made with an exposure time of 25 hr. Development of the five films of one layer line takes about $1\frac{1}{2}$ hr. and the eye-estimation of about 400 reflexions 10 hr.

In Geiger-counter measurements, each reflexion takes about 6 min., giving a total time of 40 hr. for

400 reflexions. It should be noted, however, that the time required for the very weak reflexions is much larger in the latter case and increases to 30–45 min. for such a reflexion.

Three-dimensional refinement of the structure of NH_4–H-*tartrate*

From the coordinates given in Table 1 the phases of the *hkl* reflexions were calculated, and with these phase angles and the Geiger-counter $|F_o|$ values a three-dimensional Fourier synthesis was performed. The electron density was calculated in one-quarter of the unit cell (the asymmetric unit). The atomic coordinates were determined by the method given by Megaw (1954).

In this Fourier the two aliphatic hydrogen atoms appeared as separate maxima, though the exact determination of their position gave difficulties owing to the broadness of the peaks. On the places where the bridge hydrogens were to be expected, in view of the intermolecular distance, regions of positive electron density indeed were seen to be present. For the coordinates of these hydrogen atoms the best values were chosen.

As to the hydrogen atoms of the NH_4-group, no definite positions could be determined, so we assumed the hydrogen atoms to be distributed over a sphere of radius of 1 Å. The coordinates from this Fourier are given in Table 5. Structure factors calculated with

Table 5. *Coordinates from the three-dimensional Fourier with Geiger-counter F values*

	x	y	z
O_1	0·7900	0·3845	0·3712
O_2	0·7689	0·5760	0·4500
O_3	0·4407	0·5913	0·3261
O_4	0·4328	0·4189	0·6125
O_5	0·2134	0·3605	0·2206
O_6	0·1150	0·3985	0·4779
N	0·9144	0·2170	0·0692
C_1	0·7114	0·4852	0·3915
C_2	0·5213	0·4758	0·3242
C_3	0·4205	0·3848	0·4390
C_4	0·2264	0·3811	0·3725
H_1	0·520	0·450	0·200
H_1	0·480	0·299	0·436
H_3	0·419	0·594	0·190
H_4	0·377	0·506	0·655
H_5	0·933	0·390	0·410

these coordinates and the atomic scattering factors, given in the tables of Hoerni & Ibers (1954) gave a disagreement index $R = 0{\cdot}13$ including the hydrogen atoms and $R = 0{\cdot}14$ excluding them. In this structure-factor calculation we used an isotropic temperature factor with $B = 1{\cdot}5$ Å^2.

Comparison of $|F_c|$ and $|F_o|$ showed that for five of the strongest reflexions, namely 020, 040, 310, 031 and 012, $|F_o|$ was too low, probably owing to extinction. In all our further calculations we therefore assumed for these reflexions $|F_o| = |F_c|$.

The next refinement of the atomic coordinates was performed by the method of least squares.

Minimizing the function

$$R_1 = \sum_{hkl} \{|F_o| - |F_c|\}^2,$$

and after substitution of

$$\Delta F = |F_o| - |F_c|$$

in the usual way, ε_{rj} is obtained—r denoting the atom, j (1, 2 or 3) its coordinate—:

$$\sum_{hkl} \Delta F \frac{\partial |F_c|}{\partial x_{rj}} = \sum_{hkl} \sum_{r'j'} \varepsilon_{r'j'} \frac{\partial |F_c|}{\partial x_{r'j'}} \frac{\partial |F_c|}{\partial x_{rj}} .$$

Omission of the terms

$$\frac{\partial |F_c|}{\partial x_{r'j'}} \cdot \frac{\partial |F_c|}{\partial x_{rj}} \quad \text{for} \quad r'j' \neq rj$$

gives

$$\varepsilon_{rj} = \sum_{hkl} \Delta F \frac{\partial |F_c|}{\partial x_{rj}} \Big/ \sum_{hkl} \left\{ \frac{\partial |F_c|}{\partial x_{rj}} \right\}^2 .$$

After several successive refinements, including the adjustment of the scale factor and isotropic temperature factor, the disagreement index was reduced to $R = 0{\cdot}10$.

A number of discrepancies between F_o and F_c remained, and these could not be eliminated by shifts of the atomic coordinates. At this stage we attributed to each individual atom a proper isotropic temperature factor. The temperature-factor parameters were refined by a least-squares treatment according to the formula

$$\sum_{hkl} \Delta F \frac{\partial |F_c|}{\partial B_r} = \Delta B_r \sum_{hkl} \left(\frac{\partial |F_c|}{\partial B_r} \right)^2$$

(quite analogous to the one mentioned just before). The result is given in Table 6.

Table 6. *Isotropic temperature-factor parameters*

	B (Å^2)		B (Å^2)
O_1	1·81	N	1·75
O_2	1·93	C_1	1·43
O_3	1·50	C_2	1·25
O_4	1·71	C_3	1·33
O_5	1·68	C_4	1·35
O_6	1·78		

The next three-dimensional difference Fourier gave clear indication of the anisotropic thermal motions of the atoms (Jeffrey & Cruickshank, 1953). A section of this difference Fourier is shown in Fig. 4(*a*). In the case of harmonic anisotropic vibration, the atomic scattering factor for a certain atom is given by (Cochran, 1954).

$$f = f_0 \exp\left[-2\pi^2(u_1^2 n_1^2 + u_2^2 n_2^2 + u_3^2 n_3^2) S^2\right],$$

where

f_0 = scattering factor for the atoms at rest,

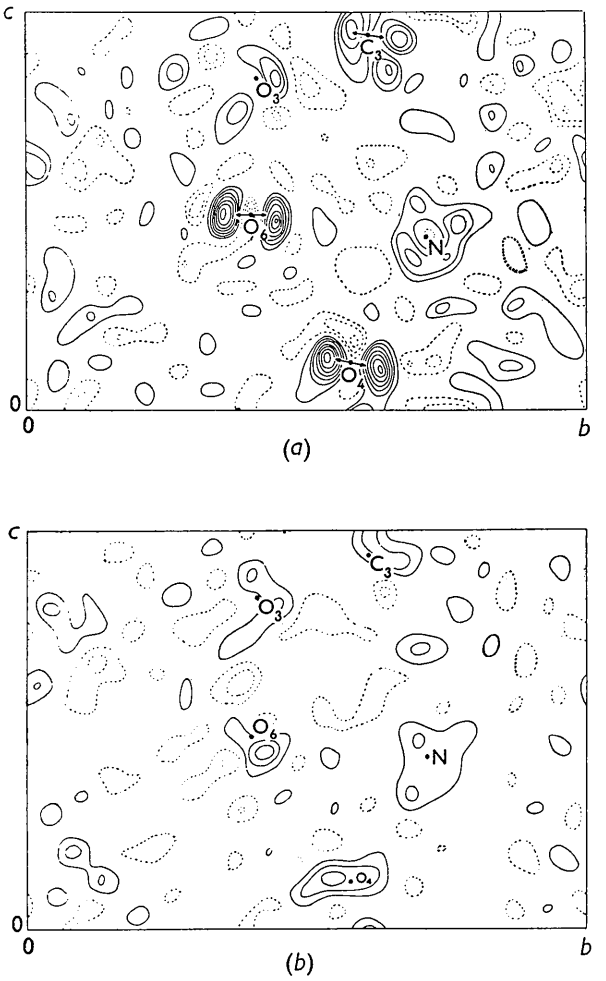

Fig. 4. (*a*) Difference Fourier section $D(\frac{5}{60}, y, z)$ before correction for the anisotropic temperature movement of the atoms. Contours are drawn at an interval of 0·1 e.Å^{-3}. Positive areas are given by full lines, negative areas by broken lines. The zero line has been omitted. (*b*) Difference Fourier section $D(\frac{5}{60}, y, z)$ after correction for the anisotropic temperature movement. Contours as in (*a*).

u_i = r.m.s. vibration amplitude in the direction of principal vibration,

n_i = direction cosine of the reflexion vector S in respect to the direction of principal vibration, $|S| = 2 \sin\theta/\lambda$.

In the case of an orthorhombic crystal this may be written

$$f = f_0 \exp \sum_i -q_i \left(\frac{h}{a} g_{i1} + \frac{k}{b} g_{i2} + \frac{l}{c} g_{i3}\right)^2 ,$$

where $q_i = 2\pi^2 \overline{u_i^2}$ and

g_{i1}, g_{i2} and g_{i3} are the direction cosines of the direction i of principal vibration in respect to the reciprocal axes a^*, b^*, c^* respectively.

For each atom the directions of the axes of the vibration ellipsoid were determined from the three-dimensional difference Fourier. The parameters q_i were determined by the method of least squares. This time we minimized the function

$$\sum_{hkl} \frac{1}{f_r} \{|F_o| - |F_c|\}^2 .$$

Neglecting cross-terms connecting different atoms, one gets for each atom three equations of the form

$$\sum_{hkl} \frac{1}{f_r} \Delta F \frac{\partial |F_c|}{\partial q_{ri}} = \sum_{hkl} \frac{1}{f_r} \sum_{i'} \frac{\partial |F_c|}{\partial q_{ri'}} \frac{\partial |F_c|}{\partial q_{ri}} \Delta q_{ri'} .$$

In order to simplify our calculations, we have initially taken the principal vibrations coincident with the *a*, *b* and *c* axes, as this proved to be nearly always the case for most atoms. In the final structure-factor calculation the actual directions, as derived from the difference Fourier maps, were introduced.

A final three-dimensional difference Fourier calculated with the parameters of Table 7 showed a maximum electron density less than 0·3 e.Å^{-3} (Fig. 4(*b*)). The electron density shows no indication of binding electrons between the atoms (Cochran, 1956).

A final least-squares refinement of the atomic coordinates, gave shifts of less than 0·003 Å. In this final stage the disagreement index had a value $R = 0{\cdot}05_5$.

The hydrogen atoms

After the refinement of the parameters of the O, C and N atoms we defined the positions of the hydrogen atoms, assigned in a former stage of the analyses.

The positions of these atoms were determined from a difference Fourier with coefficients $|F_o| - |F_c|$ in which now the contribution of the hydrogen atoms in F_c was omitted.

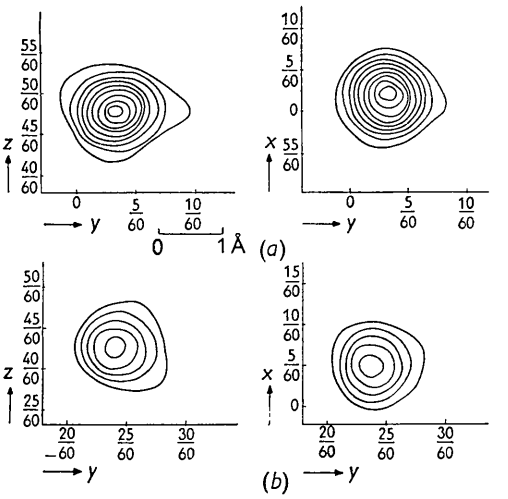

Fig. 5. Fourier sections through the centres of the hydrogen atoms. (*a*) An aliphatic hydrogen atom H_1: $D(\frac{2}{60}, y, z)$ and $D(x, y, \frac{48}{60})$. (*b*) A bridge hydrogen atom H_3: $D(\frac{5}{60}, y, z)$ and $D(x, y, \frac{43}{60})$.
Contours at an interval of 0·1 e.Å^{-3}. Zero line omitted.

Table 7. *Final atomic coordinates and temperature-factor parameters*

	x	y	z	q_1 axis	q_2 axis	q_3 axis	$4q_1$	$4q_2$	$4q_3$
O_1	0·7949	0·3835	0·3715	[100]	[021]	[01$\bar{4}$]	1·16	1·70	3·08
O_2	0·7679	0·5758	0·4526	[100]	[032]	[01$\bar{3}$]	1·42	1·90	3·20
O_3	0·4388	0·5898	0·3266	[6$\bar{1}$2]	[130]	[$\bar{1}$03]	1·42	1·49	1·54
O_4	0·4319	0·4172	0·6122	[14,1,8]	[041]	[5$\bar{1}$8]	1·66	2·63	1·19
O_5	0·2062	0·3604	0·2184	[100]	[02$\bar{1}$]	[014]	1·51	2·61	1·42
O_6	0·1085	0·3991	0·4806	[100]	[010]	[001]	0·96	3·24	1·52
N	0·9160	0·2161	0·0716	[100]	[010]	[001]	1·82	1·97	1·97
C_1	0·7078	0·4844	0·3896	[100]	[02$\bar{1}$]	[014]	0·90	1·90	1·36
C_2	0·5202	0·4749	0·3255	[100]	[010]	[001]	0·96	1·43	1·03
C_3	0·4186	0·3864	0·4376	[100]	[041]	[01$\bar{8}$]	0·96	1·49	1·49
C_4	0·2293	0·3803	0·3747	[100]	[031]	[01$\bar{6}$]	0·88	1·33	1·66
H_1	0·528	0·445	0·203					B = 2·0 Å²	
H_2	0·475	0·306	0·431						
H_3	0·417	0·600	0·195	Isotropic temperature factor					
H_4	0·378	0·506	0·645					B = 4·0 Å²	
H_5	0·931	0·395	0·400						

The xy and yz sections of this Fourier through the centres of the hydrogen atoms H_1 and H_3 are given in Fig. 5.

Comparison of the electron density in the centre of each hydrogen atom with values calculated by McDonald (1956) shows that for the atoms H_1 and H_2 a temperature factor with $B = 2{\cdot}0$ Å² and for H_3, H_4 and H_5 with $B = 4{\cdot}0$ Å² must be applied.

No clear indication of the hydrogen atoms of the NH_5 group was found, so we conclude that the original model with hydrogen atoms in a sphere of radius of 1 Å around the nitrogen atom represents a good approximation.

Bond distances and angles

The final atomic parameters, as obtained from the least-squares refinements, are given in Table 7.

From the anisotropic vibration parameters it appears that the oxygen atoms of the carboxyl groups oscillate around the C_1–C_2 and C_3–C_4 axes respectively. Cox, Cruickshank & Smith (1955) remarked that in the case of a rigid-body oscillation the time-averaged electron distribution is found towards the centre of the arc of rotation. From the vibration amplitudes we calculated for each oxygen atom of the carboxyl group a shift in the position of 0·004 Å, which has to be taken in the O_1–O_2 and O_5–O_6 directions. The corrected parameters for these atoms are given in Table 8.

Table 8. *Coordinates of the carboxyl oxygen atoms after correction for the oscillation of these groups*

	x	y	z
O_1	0·7948	0·3831	0·3714
O_2	0·7680	0·5762	0·4527
O_5	0·2064	0·3603	0·2179
O_6	0·1083	0·3992	0·4811

As to the other atoms of the tartrate ion, it appears that the anisotropic movement is not due to a rotation; for these atoms, therefore, no correction was applied.

Bond lengths and bond angles calculated from the parameters of Table 7 and Table 8 are given in Fig. 6 and Table 9 respectively.

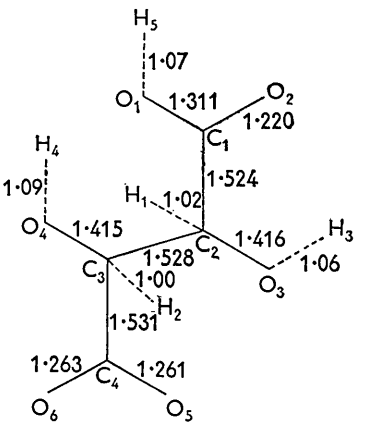

Fig. 6. Bond lengths in the tartaric acid ion.

Accuracy of the results

From the standard deviation of the observed structure-factor values, $\sigma|F_o| = 0{\cdot}4$ determined from the intensity measurements of different crystals and layer lines, we calculate for the atomic coordinates a standard deviation $\sigma(r) = 0{\cdot}001$ Å (Cruickshank, 1949).

Table 9. *Bond angles in the tartaric acid ion*

O_1–C_1–O_2	124° 29′	O_5–C_4–O_6	124° 50′
O_1–C_1–C_2	112° 28′	C_3–C_4–O_5	116° 58′
O_2–C_1–C_2	123° 3′	C_3–C_4–O_6	118° 12′
C_1–C_2–C_3	109° 28′	C_2–C_3–C_4	108° 53′
C_1–C_2–O_3	110° 29′	C_2–C_3–O_4	111° 28′
C_3–C_2–O_3	110° 24′	C_4–C_3–O_4	112° 59′
H_1–C_2–C_1	106° 16′	H_2–C_3–C_4	110° 40′
H_1–C_2–C_3	111° 6′	H_2–C_3–C_2	108° 54′
H_1–C_2–O_3	109° 6′	H_2–C_3–O_4	103° 49′
H_3–O_3–C_2	99° 14′		
H_4–O_4–C_3	114° 24′		
H_5–O_1–C_1	112° 10′		

Taking $\Delta F = |F_o| - |F_c|$ as a measure for the accuracy of the structure, we find for the atomic coordinate $\sigma(r) = 0{\cdot}002$–$0{\cdot}003$ Å and for the electron density $\sigma(\varrho) = 0{\cdot}1$ e.Å^{-3}. Hence there is no reason ot introduce more parameters in our model.

Discussion

As in the crystal structures of all tartrates, here, too, the carbon chain and the oxygen and carbon atoms of each half –CHOH–COOH of the tartraric acid molecule are nearly planar (Beevers & Hughes, 1941; Stern & Beevers, 1950; Sprenkels, 1956). From the intramolecular bond lengths and angles (Fig. 6 and Table 9) we see that the two halves of the molecule in respect to the carboxyl groups are different.

The group $C_1O_1O_2$ with distances C_1–O_1 = 1·31 Å and C_1–O_2 = 1·26 Å with O_1–C_1–C_2 = 112° 18′ and O_2–C_1–C_2 = 123° 3′ clearly is the non-ionized side of the molecule, with the longer C_1–O_1 bond due to the C–O–H group. Indeed the position of H_5 was found on the O_1 oxygen atom. The group $C_4O_5O_6$ with two equal bond lengths of 1·26 Å and O_5–C_4–C_3 = 116° 58′, O_6–C_4–C_3 = 118° 12′ is the ionized side, and is symmetrical in respect to the C_3–C_4 axis.

Calculating the double bond character from

$$R = R_1-(R_1-R_2)\frac{3x}{2x+1} \quad \text{(Pauling, 1940)},$$

where R_1 = 1·42 Å (the distance C–O), R_2 = 1·20 Å (the distance C=O), we find in the group $C_1O_1O_2$ x = 0·25 for C_1–O_1 and x = 0·75 for C_1–O_2, whereas x = 0·50 for both C_4–O_5 and C_4–O_6 in the group $C_4O_5O_6$. This is quite in agreement with the fact that in aliphatic carboxyl groups the only resonance is between

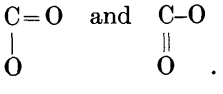

All other C–C and C–O bond lengths and angles in the molecule are normal. The C–H distance (C_2–H_1 = 1·02 Å and C_3–H_2 = 1·00 Å) is shorter than that determined from Raman spectra (1·08 Å), which gives an indication that the electron cloud does not coincide with the proton.

The crystal structure of NH_4–H-tartrate consists of layers perpendicular to the [010] direction. Layers of hydrogen-bonded tartrate ions are separated by layers of cations (Fig. 7).

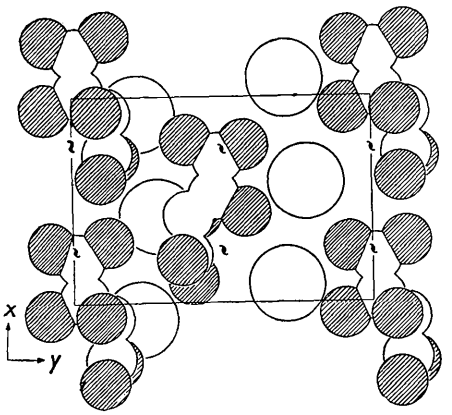

Fig. 7. The [001] projection of the cell content between z = 0 and z = ½. The whole projection can be found by the operation of the screw axes [001].

Each NH_4 ion is surrounded by eight oxygen atoms in a deformed cubic environment. The distances N–O are given in Table 10. The hydrogen bonds of one tartaric ion with its surrounding within the layer are shown in Fig. 8.

Table 10. *Nitrogen–oxygen distances*

N–O_1^{I}	3·13$_4$ Å	N–O_4^{III}	2·88$_8$ Å
N–O_5^{I}	2·96$_7$	N–O_5^{III}	2·90$_9$
N–O_2^{II}	2·85$_5$	N–O_2^{IV}	2·87$_9$
N–O_3^{II}	3·08$_9$	N–O_3^{IV}	3·15$_5$

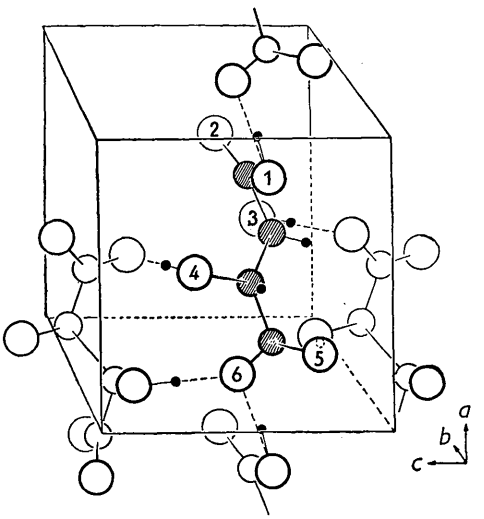

Fig. 8. Hydrogen bridges between a tartrate ion and its surroundings.

Of the non-symmetrical carboxyl-group $C_1O_1O_2$ the atom O_1 has a distance of 2·55 Å to the atom O_6 of the next ion. The distance O_1–H_5 is 1·07 Å.

The other hydrogen bonds are between the atoms O_3^{I}–O_6^{II} and O_4^{I}–O_5^{II} (molecule II arises from I by the operation of the twofold screw axis [001]):

O_3^{I}–O_6^{II} = 2·74 Å, O_3–H_3 = 1·06 Å;
O_4^{I}–O_5^{II} = 2·80^5 Å, O_4–H_4 = 1·09 Å.

In all three cases the hydrogen atoms lie near the line connecting the bonded oxygen atoms.

The structure shows a marked similarity with that of the racemic compound. In the latter there are alternately layers of D and L molecules, the D layers being identical with a layer of D-NH_4–H-tartrate.

References

Beevers, C. A. & Hughes, W. (1941). *Proc. Roy. Soc.* A, **177**, 251.
Bijvoet, J. M. (1954). *Nature, Lond.* **173**, 888.
Cochran, W. (1948). *J. Sci. Instrum.* **25**, 253.
Cochran, W. (1950). *Acta Cryst.* **3**, 268.

COCHRAN, W. (1954). *Acta Cryst.* **7**, 503.
COCHRAN, W. (1956). *Acta Cryst.* **9**, 924.
COX, E. G., CRUICKSHANK, D. W. J. & SMITH, J. A. S. (1955). *Nature, Lond.* **175**, 766.
CRUICKSHANK, D. W. J. (1949). *Acta Cryst.* **2**, 154.
GROTH, P. (1906–19). *Chemische Krystallographie*, vol. 3, p. 318. Leipzig: Engelmann.
HOERNI, J. A. & IBERS, J. A. (1954). *Acta Cryst.* **7**, 744.
JEFFREY, G. A. & CRUICKSHANK, D. W. J. (1953). *Quart. Rev. Chem. Soc., Lond.* **7**, 335.
LANGE, J. J. DE, ROBERTSON, J. M. & WOODWARD, I. (1939). *Proc. Roy. Soc.* A, **171**, 398.
MCDONALD, T. R. R. (1956). *Acta Cryst.* **9**, 162.
MEGAW, H. D. (1954). *Acta Cryst.* **7**, 771.
PAULING, L. (1940). *The Nature of the Chemical Bond*, p. 175. Ithaca: Cornell University Press.
PEERDEMAN, A. F. & BIJVOET, J. M. (1956). *Acta Cryst.* **9**, 1012.
PEERDEMAN, A. F., BOMMEL, A. J. VAN & BIJVOET, J. M. (1951). *Proc. K. Ned. Akad. Wet.* B, **54**, 16.
ROSS, P. A. (1928). *J. Opt. Soc. Am.* **16**, 433.
SPRENKELS, A. J. J. (1956). Dissertation, Utrecht.
STERN, F. & BEEVERS, C. A. (1950). *Acta Cryst.* **3**, 341.
WHITTAKER, E. J. W. (1953). *Acta Cryst.* **6**, 222.

Acta Cryst. (1958). **11**, 70

The Determination of the Coordinates of Heavy Atoms in Protein Crystals

BY W. L. BRAGG

The Royal Institution, 21 Albemarle Street, London W. 1, England

(*Received 25 September* 1957)

The paper deals with the determination of the coordinates of heavy atoms added to protein crystals. Previous methods have in general been based on Patterson or Fourier series. In the method described here, the changes in amplitude of the individual diffracted beams due to the addition of the heavy atom are plotted on a graph, from which the required coordinate can be deduced by inspection. Examples of the determination of coordinates in actual cases are given.

1. Introduction

The method of determining the phases of $F(hkl)$ values in protein crystals by the addition of heavy atoms has been established by Perutz (Green, Ingram & Perutz, 1954). He was the first to show that certain chemical groups containing a heavy atom such as mercury can be added to the molecules without appreciable alteration of crystal form, and that they produce measurable differences in the values of $I(hkl)$.

In a centrosymmetric projection, where all structure factors are real (plus or minus), the values of $\Delta F = (|F(\text{protein+heavy atom})| - |F(\text{protein})|)$ can be used to form a 'Difference Patterson'. This is so because $(\Delta F)^2 = (F(H))^2$, $F(H)$ being the structure factor of the heavy atom alone. The peaks in the Patterson indicate the approximate coordinates of the heavy atom, and from these the signs of most of the ΔF values can be ascertained. A 'Difference Fourier' can then be formed with ΔF values which gives more accurate values of the coordinates and clears up doubtful signs. A knowledge of the signs, and of the effect of the heavy atom in increasing or decreasing the intensity of each diffracted beam, enables the signs of $|F(P)|$ to be determined and a Fourier of the protein structure to be formed.

The methods outlined above can be applied only to centrosymmetrical structures. Perutz (1956) has described Fourier-series methods of dealing with the more complex cases without symmetry centres. The present note describes simple alternative ways of measuring coordinates of added heavy atoms which do not involve the use of Patterson or Fourier series and can be applied to non-centrosymmetric cases. Estimates of the coordinates so obtained are compared with those deduced by other methods. It is important to know these coordinates as accurately as possible when they are used to determine the phases of F(protein) (see, for instance, Harker (1956) and the methods described here have certain advantages as regards accuracy.

2. The determination of x and z coordinates in a monoclinic crystal

I am indebted to Dr J. C. Kendrew for letting me use some unpublished F measurements for Sperm whale myoglobin Type A, determined in the course of an investigation directed towards a three-dimensional Fourier of the structure. They are measurements of $|F(hk0)|$ and $|F(0kl)|$ for

myoglobin,
myoglobin+parachloromercuri-benzenesulphonic acid, PCMBS,
myoglobin+mercury diammine, $HgAm_2$,
myoglobin+gold chloride, Au.

The space group and cell constants are